A precipitation isotopic response in 2014-2015 to moisture transport changes in the central Himalayas

Josefine Axelsson[1], Jing Gao[2,3], Sabine Eckhardt[4], Massimo Cassiani[4], Deliang Chen[5] and Qiong Zhang[1]

[1] Department of Physical Geography and the Bolin Centre for Climate Change, Stockholm University, 106 91 Stockholm, Sweden

[2] State Key Laboratory of Tibetan Plateau Earth System, Resources and Environment, Institute of Tibetan Plateau Research, Chinese Academy of Sciences, Beijing 100101, China

[3] Lanzhou University, Lanzhou 733000, China

[4] Norwegian Institute for Air Research (NILU), 2027 Kjeller, Norway

[5] Department of Earth Sciences, Gothenburg University, 405 30 Gothenburg, Sweden

Corresponding authors: J. Axelsson (josefine.axelsson@natgeo.su.se)

Key Points:

- Direct measurements of event-based $\delta^{18}O$ and d-excess in precipitation in the central Himalayas in the 2015 monsoon season compared to 2014.
- Combination of in-situ isotopic measurements with simulations of evaporation minus precipitation (E-P) using FLEXPART.
- Isotopic variations in precipitation are associated with changes in moisture supplies along the transport path.

Abstract

The impact of moisture transport and sources on precipitation stable isotopes ($\delta^{18}O$ and d-excess) in the central Himalayas are crucial to understanding the climatic archives. However, this is still unclear due to the lack of in-situ observations. Here we present measurements of stable isotopes in precipitation at two stations (Yadong and Pali) in the central Himalayas during 2014-2015. Combined with simulations from the dispersion model FLEXPART, we investigate effects on precipitation stable isotopes related to changes in moisture sources and convections in the region, and possible influence by El Niño. Our results suggest that the moisture supplies related to evaporation over northeastern India and moisture losses related to convective activities over the Bay of Bengal (BoB) and Bangladesh region play important roles in changes in $\delta^{18}O$ and d-excess in precipitation in the Yadong valley. Outgoing longwave radiation and moisture flux divergence analysis further confirm that the contribution from continental evaporation dominates the moisture supply in the central Himalayas with a lesser contribution from convection over the BoB during the 2015 monsoon season compared with 2014. A change in the altitude effect is observed in 2015, which is more significant than the temperature and precipitation amount effect during the observation period. These findings provide valuable insights into climatic interpretations of paleo-isotopic archives with an isotopic response to changes in moisture transport to the central Himalayas.

Plain Language Summary

Evaporation, convection, temperature, topography, large-scale circulation (Indian summer monsoon and westerlies), and large-scale modes (e.g., ENSO) all play roles in precipitation variability in the Himalayas. Influences of processes related to these factors are not well understood, and therefore difficult to interpret climatic signals in paleo-climate records. Stable isotopes in precipitation are useful tools to trace different moisture sources and convective activities along the transport. Therefore, we present measurements of stable isotopes in precipitation at two stations in the central Himalayas during 2014 and 2015 to estimate changes in moisture sources and convection. To do so, we also use the dispersion model FLEXPART to diagnose changes in moisture supplies and losses along transports during 2015 compared to 2014. We found that there is less moisture supply from the BoB in 2015, and more from the Indian continent with spatiotemporal variations.

1 Introduction

The Indian summer monsoon (ISM) is an integral component of the Asian monsoon system and brings heavy rainfall to the southern Tibetan Plateau (TP) from May/June to September (Feng & Zhou, 2012; Wu et al., 2017; Ya et al., 2013; Yao et al., 2013), which is crucial for water supply to nearly 1.9 billion people in immediate regions (ICIMOD, 2021). The ISM is driven by the land-sea thermal gradient (Ananthakrishnan, 1970; Chen et al., 2022; Clark et al., 2000) and the elevated heat source from the TP during the monsoon season (Hahn & Manabe, 1976; Ding & Chan, 2005; Hao et al., 2013). Moisture is mainly transported to the southern TP from the Bay of Bengal (BoB) and the Arabian Sea, with the latter recycled over the Indian continent before encountering the Himalayas (Chen et al., 2012; Feng & Zhou, 2012; Zhang et al., 2017). The ISM creates extreme precipitation along the southern Himalayas due to the "barrier effect" (Hahn & Manabe, 1976; Wang & Chang, 2012), impacting river discharge and glacier melting (Gao et al., 2019). Large-scale climate variability modes, such as El Niño Southern Oscillation (ENSO), modulate the ISM in different timescales (Cai et al., 2017; Gao et al., 2018; Kripalani & Kulkarni, 1997; Srivastava et al., 2019; Torrence & Webster, 1999; Webster, 1995). For instance, a drier monsoon season over the Indian Peninsula was observed together with a weakened monsoon circulation during the strong El Niño event of 2015 (Kakatkar et al., 2018; Mekonnen et al., 2016; Power et al., 2021). However, the impact on precipitation variability in complex topography like the Himalayas is underrepresented in studies due to the scarcity of observational data.

Stable isotopes in precipitation ($\delta^{18}O$ and δD) serve as valuable tracers for moisture sources and transport processes (Araguás-Araguás et al., 2000; Dansgaard, 1964; Gao et al., 2011). During water phase changes, such as evaporation and condensation, isotopic fractionation leads to the enrichment or depletion of stable isotopes in each phase (Craig, 1961; Dansgaard, 1964). Long-term monitoring of stable isotopes in precipitation on the TP has revealed a regional complexity driven by geographical and meteorological factors, including local climatic variables such as surface air temperature and precipitation amount (Craig, 1961; Dansgaard, 1964; Merlivat & Jouzel, 1979; Rozanski et al., 1992), and the regional atmospheric circulations related to the conditions at the moisture source and transports of the precipitated water (Araguás-Araguás et al., 2000; Rozanski et al., 1993). Local conditions affecting the precipitation can be distinguished

through the temperature, precipitation amount, and altitude effect. The temperature effect is caused by an accumulation of ^{18}O due to an increase in evaporation, whereas the precipitation amount effect is enriched isotopic composition through condensation while the remaining vapor is depleted of ^{18}O (Dansgaard, 1964; Gat, 1996; Rozanski et al., 1992). In the monsoon region of the TP (<30°N), the precipitation amount effect dominates at the seasonal scale (Yao et al., 2013). Orographic uplift of air masses, typical of high elevations such as the Himalayas, also gradually depletes ^{18}O with increasing altitude due to orographic condensation and rainout (Acharya et al., 2020; Dansgaard, 1964; Ambach et al., 1968; Gonfiantini et al., 2001).

The second-order stable isotope parameter, deuterium excess (d-excess=$\delta D-8*\delta^{18}O$), can provide additional information to evaluate the condition of moisture sources, such as relative humidity, sea-surface temperature, and wind speed during evaporation (Clark & Fritz, 1997; Dansgaard, 1964; Merlivat & Jouzel, 1979). Evaporation from humid sources will associate with low d-excess in the later precipitated water, and vice versa (Gat, 1996; Merlivat & Jouzel, 1979; Rozanski et al., 1993). d-excess is also found to increase through continental moisture recycling and decrease through re-evaporation of droplets during precipitation events (Bershaw, 2018; Gat, 1996; Tian et al., 2001, 2005). More studies suggest that besides the local convection, the moisture transports and sources driven by large-scale atmospheric circulation, such as the westerlies and ISM, also play important roles in variations of precipitation stable isotopes around the southern TP (Acharya et al., 2020; Adhikari et al., 2020; Dai et al., 2021; Ren et al., 2017). Precipitation stable isotopes are positively correlated to outgoing longwave radiation over the south of the Himalayas (Adhikari et al., 2020; He et al., 2015) and negatively correlated to high-level cloud cover (Wang et al., 2020), suggesting that convective activity regulates the depletion of the heavier isotopes.

A strong El Niño event was identified in 2015, which resulted in a drier monsoon season over the Indian Peninsula together with a weakened monsoon circulation (Kakatkar et al., 2018; Mekonnen et al., 2016; Power et al., 2021). Thus, we suppose that this event could impact precipitation and stable isotopes in precipitation in the central Himalayas. Here we present event-based precipitation stable isotope measurements from Yadong and Pali stations in the central Himalayas during 2014-2015. Using the FLEXPART model we aim to understand changes in

moisture sources and convection, as well as their impacts, on precipitation stable isotopes in the region. We first provide an overview of the in-situ observations and the FLEXPART model. We then present the spatiotemporal changes of the observed stable isotopes in precipitation at Yadong and Pali in 2014 and 2015, along with the possible controls of precipitation stable isotopes by local climates. In subsequent sections, we examine variations of moisture source origins and convective activities associated with variations in stable isotopes in precipitation in Yadong Valley before and during the strong El Niño event in 2015. Finally, we conclude our study.

2 Data and Methods

2.1 Study area and measurements of precipitation stable isotopes

Yadong and Pali stations are located within Yadong Valley in the central part of the Himalayas (Fig. 1a), with an altitude difference of 1355 m.a.s.l.. Southwesterly winds dominate from June to September, which transports high-humidity air from the BoB and Arabian Sea to the north, resulting in the majority of the annual precipitation (Feng & Zhou, 2012; Wu et al., 2017; Ya et al., 2013; Yao et al., 2013). Specific humidity increases with altitude at 500 hPa but decreases at 850 hPa (Fig. 1b and 1c). Temperature increases through spring and summer, with Yadong experiencing higher temperatures than Pali due to its lower altitude (Fig. 2). The two stations differ in annual temperature and total precipitation amount by 6.3°C and 343 mm, respectively, during the sampling period. In this study, 125 samples have been utilized from Yadong and 130 from Pali, obtained from the Tibetan Network for Isotopes in Precipitation (TNIP) between 13 March 2014 and 23 July 2015 (Tab. 1).

135 **Table 1.** Summary of the climatic and sampling information at Yadong and Pali stations in this
136 study. Tot P is the total precipitation during the sampling period, Avg P is the average amount of
137 precipitation per precipitation event, and Avg T is the average temperature on days with
138 precipitation during the sampling period.

Station	Latitude	Longitude	Altitude (m.a.s.l.)	Sampling period	Samples (n)	Tot P (mm)	Avg P (mm/day)	Avg T (°C)
Yadong	27° 29' 40" N	88° 55' 01" E	2945	2014-03-13 – 2015-07-18	125	854.1	6.8	10.9
Pali	27° 43' 16" N	89° 09' 08" E	4300	2014-03-18 – 2015-07-23	130	510.9	3.9	4.6

139

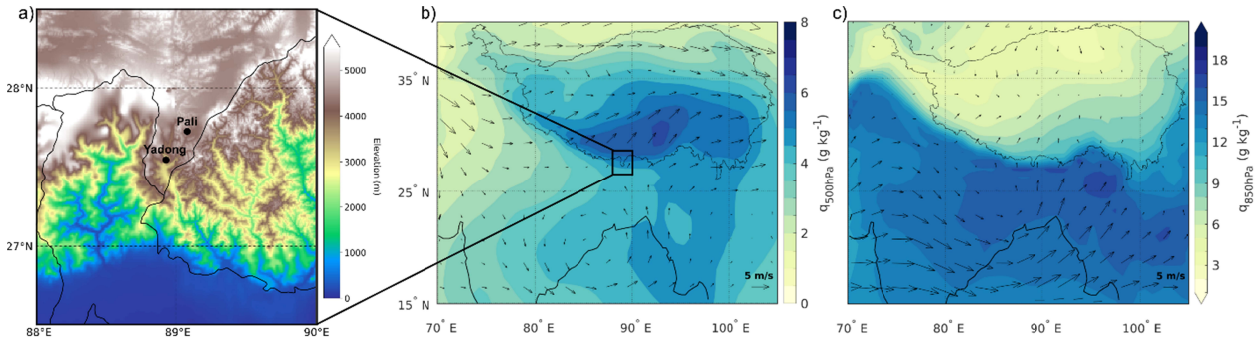

140

141 **Figure 1**. Locations of the Yadong and Pali stations and topography (a), June-September specific
142 humidity and mean wind at 500 hPa (b) and 850 hPa (c). Wind and specific humidity are
143 retrieved from ERA-Interim (Dee et al., 2011), and topographical information is from ETOPO1
144 (Amante & Eakins, 2009; NOAA National Geophysical Data Center, 2009).
145
146 The precipitation samples were collected after each precipitation event, and air temperature and
147 precipitation amounts were also recorded. After each precipitation event stopped, water samples
148 were immediately sealed into dry and sterile 15-milliliter polyethylene bottles. Until analysis, the
149 samples were stored in cold closets. For snowfall events, the samples were first melted in a
150 sealed plastic bag at room temperature before being transferred into the bottles. The oxygen and
151 hydrogen isotopic ratios ($\delta^{18}O$ and δD) of the samples were measured in the Key Laboratory of

Tibetan Environment Change and Land Surface Processes, CAS, using a cavity ring-down spectroscopy (Picarro-2130i Liquid Water Isotope Analyzer) with a precision of ±0.1‰ for $\delta^{18}O$ and ±0.4‰ for δD. Oxygen isotope composition is usually reported in the δ-notation as

$$\delta^{18}O = \left(\frac{\frac{^{18}O}{^{18}O_{sample}}}{\frac{^{18}O}{^{18}O_{standard}}} \right) \times 1000(‰), \qquad (1)$$

against the Vienna Standard Mean Ocean Water (V-SMOW, Dansgaard, 1964; Kendall and Caldwell, 1998). The Indian summer monsoon season is defined as June to September (JJAS), following previous studies (Gao et al., 2015, 2016; Yao et al., 2013), and other months are presented either as non-monsoon (October-May) or pre-monsoon (March-May) seasons.

2.2 Reanalysis data

ERA-interim data have been widely used to diagnose changes in moisture over the TP (Gao et al., 2014), and have proven to perform well in the Himalayas (Nogueira, 2020). We used zonal wind regimes (u and v), specific humidity (q), and the vertical integral of the divergence of moisture flux at 500 and 850 hPa (Dee et al., 2011). The data was retrieved with 0.75° × 0.75° resolution during 1986-2015 and JJAS 2014 as well as 2015. A climatology was provided during JJAS 1986-2015.

Satellite-based measurements of outgoing longwave radiation (OLR) provide a valuable proxy for deep atmospheric convection conditions in the tropics (Evans & Webster, 2014; Krishnan et al., 2000; Risi et al., 2008; Zhang, 1993). We use daily interpolated OLR data with the horizontal resolution of 1°×1° provided by NOAA/OAR/ESRL PSL (Liebmann & Smith, 1996) during 1986-2015, JJAS 2014 and 2015. Anomalies are calculated relative to the 1986-2015 climatology using averaged daily measurements.

2.3 FLEXPART model

We use the FLEXible PARTicle dispersion model (FLEXPART), a Lagrangian dispersion model (Pisso et al., 2019; Stohl et al., 1998; Stohl & James, 2004, 2005) to calculate back trajectories of air parcels to determine the surface moisture flux through evaporation (*E*) minus precipitation (*P*) before and during the monsoon seasons of 2014 and 2015. This model is widely applied to estimate long-distance and mesoscale dispersion of air pollutants and chemicals (Stohl et al.,

1998), and analyze the global and regional moisture flux (Drumond et al., 2011; Gimeno et al., 2010; Sodemann & Stohl, 2013; Stohl et al., 2008; Stohl & James, 2004, 2005; Sun & Wang, 2014). Furthermore, by adding a criterion for precipitation threshold (-0.5 mm 3 h^{-1}), particles contributing to a precipitation event can be traced back, relying on wind fields calculated by horizontal and vertical wind components, air temperature, and specific humidity (Pisso et al., 2019).

For diagnostics on the surface moisture flux divergence over an area (A), E-P for the total particles residing over A is given by

$$E - P \approx \frac{\sum_{k=1}^{K}(e-p)}{A} \qquad (2)$$

where K is the number of N particles that resides over A, and e-p is the rate of moisture change along the trajectory (Stohl & James, 2004). With instantaneous rates of evaporation ($E_i = E - P$ when $E - P > 0$) and precipitation ($P_i = P - E$ when $E - P < 0$), $E - P$ can be diagnosed for every evaluation interval (Stohl & James, 2004; Trenberth et al., 2003).

In this study, the air mass is divided homogeneously between dispersed particles. The particles are advected by the wind fields retrieved from ERA-interim, as well as turbulent and convective motions, with 6-hourly analyses (at 00.00, 06.00, 12.00, and 18.00 UTC), and 3-hourly forecasts at intermediate times (at 0300, 0900, 1500, and 2100 UTC), with 1° × 1° spatial resolution covering 60 vertical levels from 0.1 to 1012 hPa (Dee et al., 2011). For each day with a precipitation event at either Yadong or Pali station, the particles are backtracked for 8 days. The release grid is set around Yadong and Pali stations at latitudes 27-28° and longitudes 88.5-89.5°. To better evaluate the evaporation component, we used the method of Michel et al. (2021) and considered only particles in the planetary boundary layer (PBL) for moisture uptake.

3 Results and discussion

3.1 Observed characteristics of precipitation stable isotopes at Yadong valley

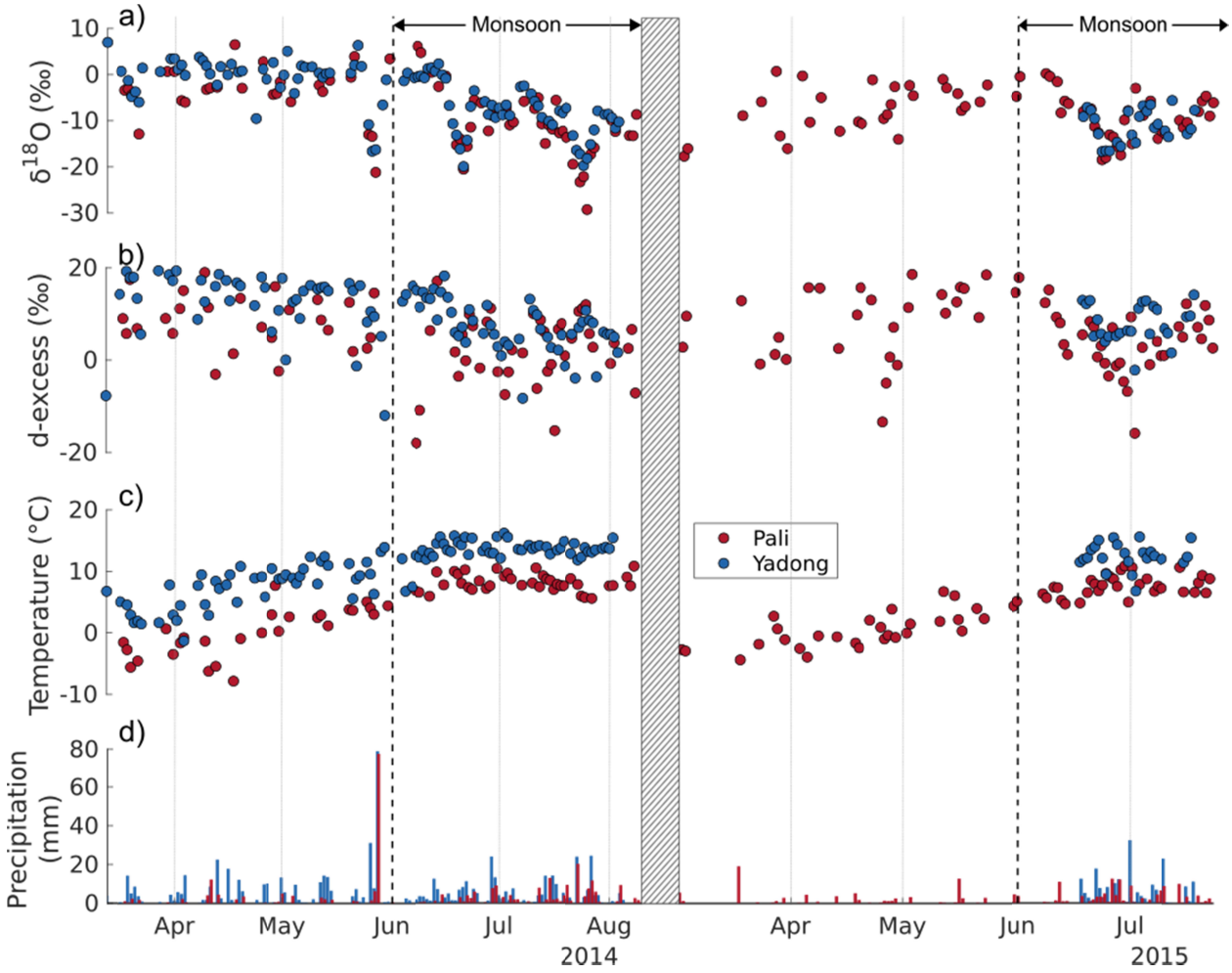

Figure 2. Temporal variations in (a) $\delta^{18}O$, (b) d-excess, (c) temperature, and (d) precipitation amount from 13 March 2014 to 23 July 2015 at Yadong (blue) and Pali (red) stations in Yadong valley. The striped patch represents a break period in sampling between 11 August 2014 to 1 March 2015, and dashed lines indicate 1 June for each year.

A pronounced seasonality of temperature and stable isotopes in precipitation are observed at Yadong and Pali. The temperature at both sites exhibits seasonal variations with a gradual increase from April to August 2014 (Fig. 2c). In April, the average temperature is 6.4°C at Yadong and -1.6°C at Pali, while in August it reaches 14.2°C at Yadong and 8.5°C at Pali. In

June and July 2015, the average temperature is approximately 0.7°C lower compared to 2014. Precipitation amount at Yadong shows a decrease during the pre-monsoon and monsoon seasons in 2015 compared to 2014 (Fig 2d). The stable isotopes in precipitation at Yadong shows significant daily fluctuations and seasonal variations during the observation period (Fig. 2). A pronounced decrease of $\delta^{18}O$ and d-excess at both stations appears from June to August, which corresponds to the maturing of the monsoon (Yao et al., 2013).

The average $\delta^{18}O$ value at Yadong is -0.62‰ during the pre-monsoon season (March to May 2014), whereas the average drops significantly to -7.59‰ during the monsoon season. There are two notable low points during the monsoon season, with $\delta^{18}O$ values of -19.92‰ on 22 June and -19.76‰ on26 July. These low points align closely with days of heavier precipitation. It is observed that the $\delta^{18}O$ range in 2015 (-16.66 to -5.61‰) is smaller than in 2014 (-19.92 to 2.35‰). The average $\delta^{18}O$ value during the overlapping months is 3.76‰ lower in 2015. The d-excess values exhibit similar seasonal characteristics, with higher values during the pre-monsoon and lower values during the monsoon season (Fig. 2b). In 2014, the mean d-excess at Yadong is 13.13‰ during pre-monsoon and 7.56‰ during the monsoon season. The minimum d-excess value of -12.04‰ occurs in May, while the maximum value of 22.68‰ occurs in April. It is worth noting that the relationship between low $\delta^{18}O$ and higher d-excess is more pronounced during the monsoon season in 2014 compared to 2015 (Fig. 2 and 3c, d). These variations in d-excess and $\delta^{18}O$ indicate that different moisture sources contribute to precipitation at Yadong during the pre-monsoon and monsoon seasons. Such seasonal variations are related with the changes to the dominant moisture transport that is discussed in section 3.3.

The stable isotopes in precipitation at Pali show similar seasonal characteristics to those at Yadong in 2014 (Fig. 2a, b). However, the range of d-excess is larger at Pali in the 2015 monsoon season compared to 2014. It is noticed that lower values of $\delta^{18}O$ and d-excess are observed at Pali, and there are three extremely low values of $\delta^{18}O$ observed from 26 to 28 May 2014, which align with the low values at Yadong. This suggests the presence of an altitude effect and indicates that the same rainfall process is occurring at both stations.

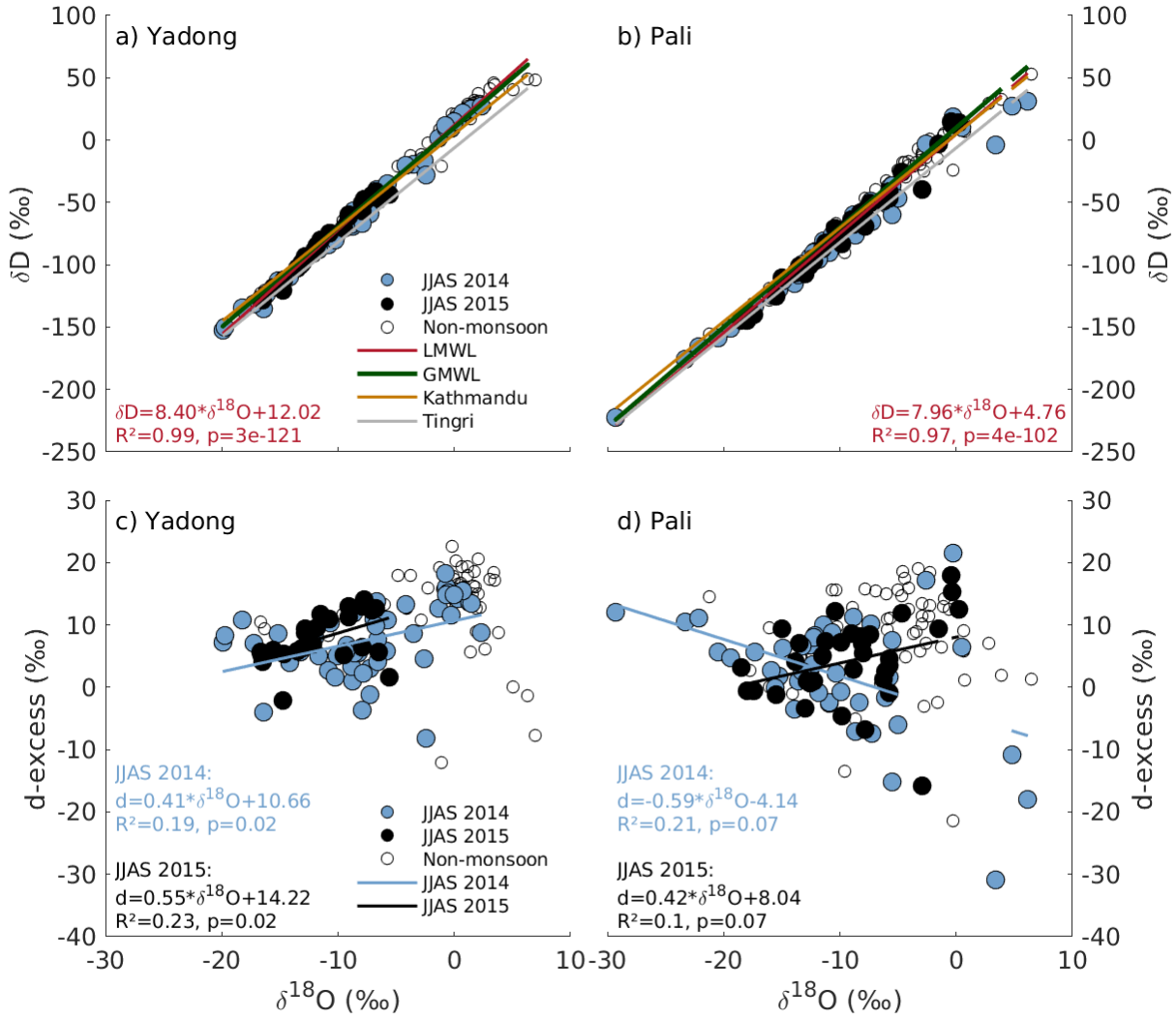

Figure 3. Relationships between event-based $\delta^{18}O$ and δD at Yadong (a) and Pali (b). The local meteoric water line is displayed in red for both stations, while the GMWL (green line), Kathmandu LMWL (orange line, (Adhikari et al., 2020)) and Tingri LMWL (grey line, (Yu et al., 2016)) are presented as reference lines. The $\delta^{18}O$-d-excess-relationship is shown for Yadong (c) and Pali (d). Linear regression (lines) and precipitation stable isotopes (filled circles) are displayed for JJAS 2014 (light blue) and JJAS 2015 (black).

Table 2. Local meteoric water line (LMWL) for Yadong and Pali, including coefficient of determination (R^2) and p-value. The LMWL is calculated for the entire sampling period and the events corresponding to the monsoon season of 2014 and 2015.

Station	Period	LMWL	R^2	p

Yadong	All events	$\delta D = 8.4 \times \delta^{18}O + 12.02$	0.99	<0.01
	2014 June-August	$\delta D = 8.4 \times \delta^{18}O + 10.66$	0.99	<0.01
	2015 June-July	$\delta D = 8.6 \times \delta^{18}O + 14.22$	0.99	<0.01
Pali	All events	$\delta D = 7.96 \times \delta^{18}O + 4.76$	0.97	<0.01
	2014 June-August	$\delta D = 7.4 \times \delta^{18}O - 4.14$	0.98	<0.01
	2015 June-July	$\delta D = 8.4 \times \delta^{18}O + 8.04$	0.98	<0.01

The local meteoric water line (LMWL) is defined by the linear relationship between $\delta^{18}O$ and δD in precipitation at local or regional scales relative to the global meteoric water line (GMWL) (Clark & Fritz, 1997; Dansgaard, 1964; Gao et al., 2011; Ren et al., 2017). In Yadong, the slopes and intercepts of the LMWL during the observational period and monsoon seasons are slightly higher than those of the GMWL (Fig. 3a and Tab. 3). This suggests similar moisture source characteristics in 2014 and 2015 (Craig, 1961). In the 2014 monsoon season at Pali, the LMWL exhibits the lowest slope (7.4) and intercept (-4.14), deviating significantly from the GMWL and LMWLs at Yadong (Tab. 3). This indicates the influence of more humid moisture sources and sub-cloud evaporation of raindrops at Pali (Merlivat & Jouzel, 1979). Contrarily, the LMWL at Pali during the 2015 monsoon season reflects similar moisture source conditions to those at Yadong (Tab 3). It is noticed that the LMWLs at Yadong and Pali during the observation period closely resemble the LMWL at Kathmandu (Nepal), which is located west of Yadong Valley at an elevation of 1400 m.a.s.l. and has an average annual temperature of 18.8°C (Yu et al., 2016). However, they differ significantly from the LMWL at Tingri (Tibet), situated northwest of Yadong Valley at an elevation of 4322 m.a.s.l., with an average annual temperature of 3.3°C (Yu et al., 2016) (Fig. 3a, b). This indicates similar moisture sources but with distinct local kinetic effects.

The linear correlation between $\delta^{18}O$ and d-excess during the monsoon seasons is shown in Fig. 3c and d. Yadong has significantly positive slopes in both 2014 and 2015 (Fig. 3c). The slope at Pali in 2015 is similar to that at Yadong, despite a 1355-meter difference in altitude between the two stations (Fig. 3d). This suggests that there was a higher proportion of mixing at both stations in 2015. These observations may be linked to changes in convection activities, as discussed in section 3.3.

3.2 Influences of local and regional processes

An altitude effect between Yadong and Pali is observed during the sampling period. The increase in altitude of 1355 meters leads to a lower monsoonal $\delta^{18}O$ at Pali by -1.10‰ during overlapping sampling months of June-July, resulting in an altitudinal lapse rate of -0.08‰/100m. In the 2014 monsoon season, the lapse rate is found to be -0.22‰/100m, whereas in 2015 it is 0.14‰/100m. The 2014 values are more consistent with those reported by Acharya et al. (2020) in Nepal (-0.19‰/100m) than the combined 2014-2015 or 2015 lapse rates. Moisture transported by either ISM or westerlies first reaches Yadong and is subsequently uplifted to Pali, leading to modifications in $\delta^{18}O$ due to kinetic fractionation (Cai et al., 2017). During 2015, precipitation $\delta^{18}O$ at Pali tends to be higher with larger positive anomalies, which is consistent with findings by Wang et al. (2020) and Cai et al. (2017) in El Niño years. Furthermore, the higher temperature and d-excess at Yadong indicate stronger local evaporation than at Pali.

The altitude effect is relevant to changes in local temperature and precipitation amount. Significant negative correlations between $\delta^{18}O$ and temperature are observed during the sampling period at both stations (Yadong: R= -0.48, Pali: R= -0.28). However, this relationship is weaker at Pali and is not observed in separate monsoon seasons for either station. Similar findings have been confirmed in Kathmandu and Tingri, where only the daily events (Adhikari et al., 2020) or the winter season showed a relationship to temperature (Chhetri et al., 2014; Yu et al., 2016). On a daily scale, weak but significant negative correlations exist between precipitation amount and $\delta^{18}O$ at both stations (Yadong: R= -0.28, Pali: R= -0.37), with particularly strong correlations observed at Pali during the 2014 (R = -0.51) and 2015 (R = -0.52) monsoon seasons.

Thus, we suggest that local effects related to temperature and precipitation amount are not the main drivers of changes in precipitation stable isotopes in the Yadong Valley during 2014 and 2015. The differences in the relationships between isotopes and local processes during the monsoon seasons of those years may indicate the influence of ENSO-related moisture transport on precipitation stable isotopes in Yadong Valley at the regional scale.

3.3 Temporal variations of moisture flux and convective activities

To investigate the impact of moisture transport on precipitation stable isotopes in Yadong Valley, we calculated net moisture flux divergence (E-P) over Yadong Valley (27-28°N, 88.5-89.5°E) during days with measured precipitation using FLEXPART. Due to the coarser resolution of the reanalysis data (1°) and the short distance between the two stations, we analyze the back trajectories from the same initiating grid for both stations. Positive values indicate a net moisture supply, while negative values indicate moisture loss from the air mass. We analyzed days that correspond to $\delta^{18}O$ and d-excess values ≤25 percentile or ≥75 percentile of their distributions (Tab. 4) in June-August 2014 and 2015. The observed values at Yadong and Pali suggest that different moisture sources modulate the precipitation stable isotopes in Yadong Valley, especially in 2015. The diagnosed E-P corresponds similarly to $\delta^{18}O$ and d-excess for the same quartiles, thus, we only present results of d-excess, which efficiently reflects source conditions (Fig. 4).

Table 3. Lower and upper quartiles of $\delta^{18}O$ and d-excess distributions during June-August in 2014 and 2015, and the number of events in each quartile (*n*).

		2014		2015	
		≤25 pc (*n*)	**≥75 pc (*n*)**	**≤25 pc (*n*)**	**≥75 pc (*n*)**
$\delta^{18}O$	**Yadong**	-10.81‰ (*13*)	-1.64‰ (*12*)	-13.79‰ (*6*)	-7.88‰ (*6*)
	Pali	-15.06‰ (*9*)	-5.66‰ (*9*)	-12.80‰ (*9*)	-5.74‰ (*9*)
d-excess	**Yadong**	4.72‰ (*13*)	12.52‰ (*12*)	5.60‰ (*6*)	11.83‰ (*6*)
	Pali	-2.42‰ (*10*)	8.55‰ (*9*)	0.74‰ (9)	8.42‰ (*9*)

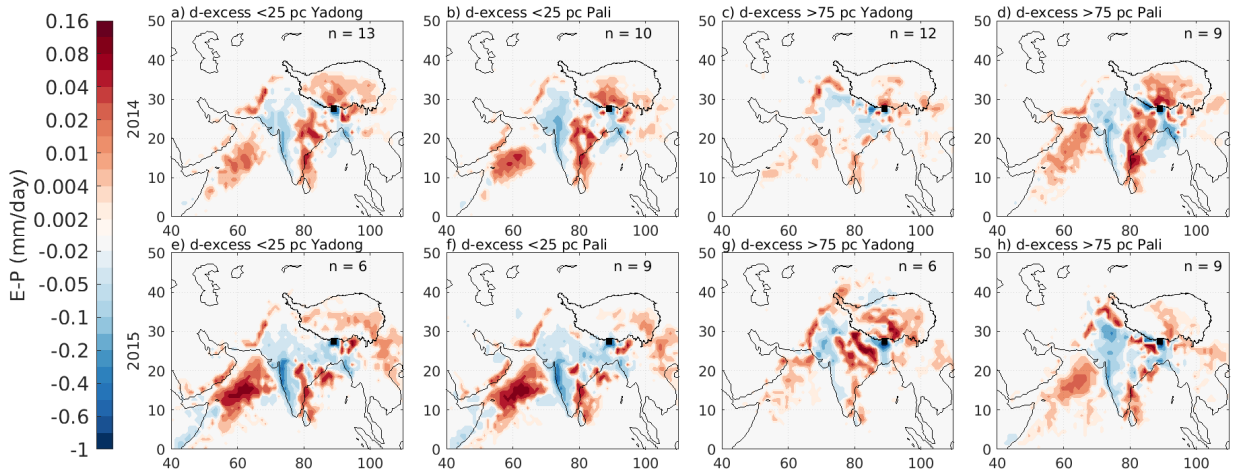

Figure 4. E-P as mm per 24 hours, diagnosed from 8-day back-trajectories based on residence within the PBL for sampled precipitation events. Events are analyzed based on extremes in d-excess (e.g., ≤25 and ≥75 percentile) for each station and year, where *n* is number of extreme events identified and simulated.

The E-P results reveal variable contributions of moisture originating from the western Arabian Sea, the eastern Indian Peninsula, the Himalayas, and the western BoB in 2014 and 2015 (Fig. 4). E-P over Bangladesh and western and northern India exhibit negative values, indicating moisture loss during transport towards Yadong Valley. In 2015, the moisture source and loss regions differ between low d-excess events (⩽25 percentile of d-excess distributions) and high d-excess events (⩾75 percentile of d-excess distributions) at Yadong (Fig. 4e, g). The latter receives more moisture from northern and central India as well as the southern TP, and less from the Arabian Sea, compared with the former. This suggests that the direct contributions of recycling over the Indian continent prior to the central Himalayas precipitation event cannot be ignored. Meanwhile, further negative E-P in Bangladesh and over the BoB are identified.

Similar characteristics are found at Pali. In 2015, significantly less moisture supply over eastern India and southern TP to Pali together with stronger moisture supply from the Arabian Sea are observed for all extreme d-excess events compared to 2014 (Fig 4b, d, f, h). Additional negative E-P in Bangladesh is also diagnosed in 2015. These changes correspond with depleted $\delta^{18}O$ and

346 d-excess at Yadong and Pali, which are consistent for stable isotopes in precipitation undergoing
347 long-distance transport and increased contribution from wet sources (Gao et al., 2013).
348

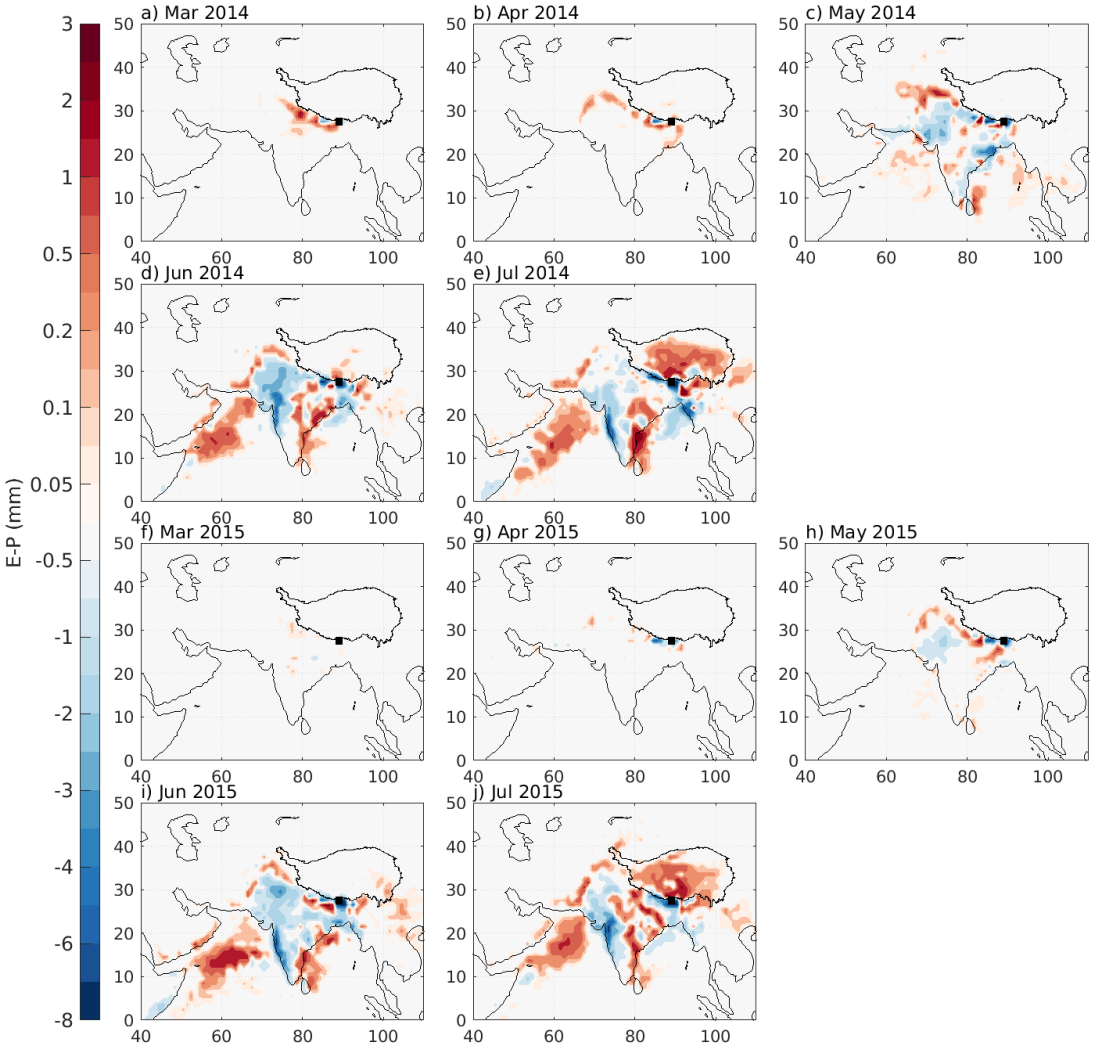

349

350 **Figure 5.** Monthly E-P as millimeters, diagnosed from 8-day back-trajectories based on
351 residence within the PBL for sampled precipitation events at either of the stations in March-July
352 (a-e) 2014, and (f-j) 2015. The target domain (27-28°N, 88.5-89.5°E) is marked as a black box
353 covering both Yadong and Pali stations.
354

355 To examine the impacts of upstream convective activities before moisture is transported to the
356 Yadong Valley, we grouped the measured precipitation events into months for 2014 and 2015
357 and calculated E-P (Fig. 5). At a monthly scale, a clear shift in moisture sources between 2014

and 2015 is evident based on E-P along moisture transport paths. From March to May, less moisture from northern India, the Arabian Sea, and the BoB contribute to precipitation events in the Yadong Valley in 2015, while more positive E-P is found over the Indian continent, compared to 2014. It is noticed that the negative E-P over eastern India observed in June 2015 turns to positive in 2014 (Fig. 5d, i). However, it shifts to a strong moisture supply (positive E-P) in July 2015, which is associated with enriched $\delta^{18}O$ and d-excess at Yadong and Pali (Fig. 2a). Reanalysis data over Bhutan confirms the temporal and spatial variability of ISM precipitation amount during July 2015 (Power et al., 2021).

To better understand the variations of monsoon moisture transport to Yadong Valley during 2015 compared to 2014, we analyzed the vertically integrated moisture flux divergence and zonal wind at 850 hPa. Figure 6 displays the anomalies in 2014 and 2015 zonal winds at 850 hPa and vertically integrated moisture flux divergence, relative to the climatology of 1986-2015. We observed strong zonal winds and a moisture divergence in the western Indian Ocean, accompanied by moisture convergence along the west coastline of India, the BoB, and the southern margin of the TP (Fig 6a).

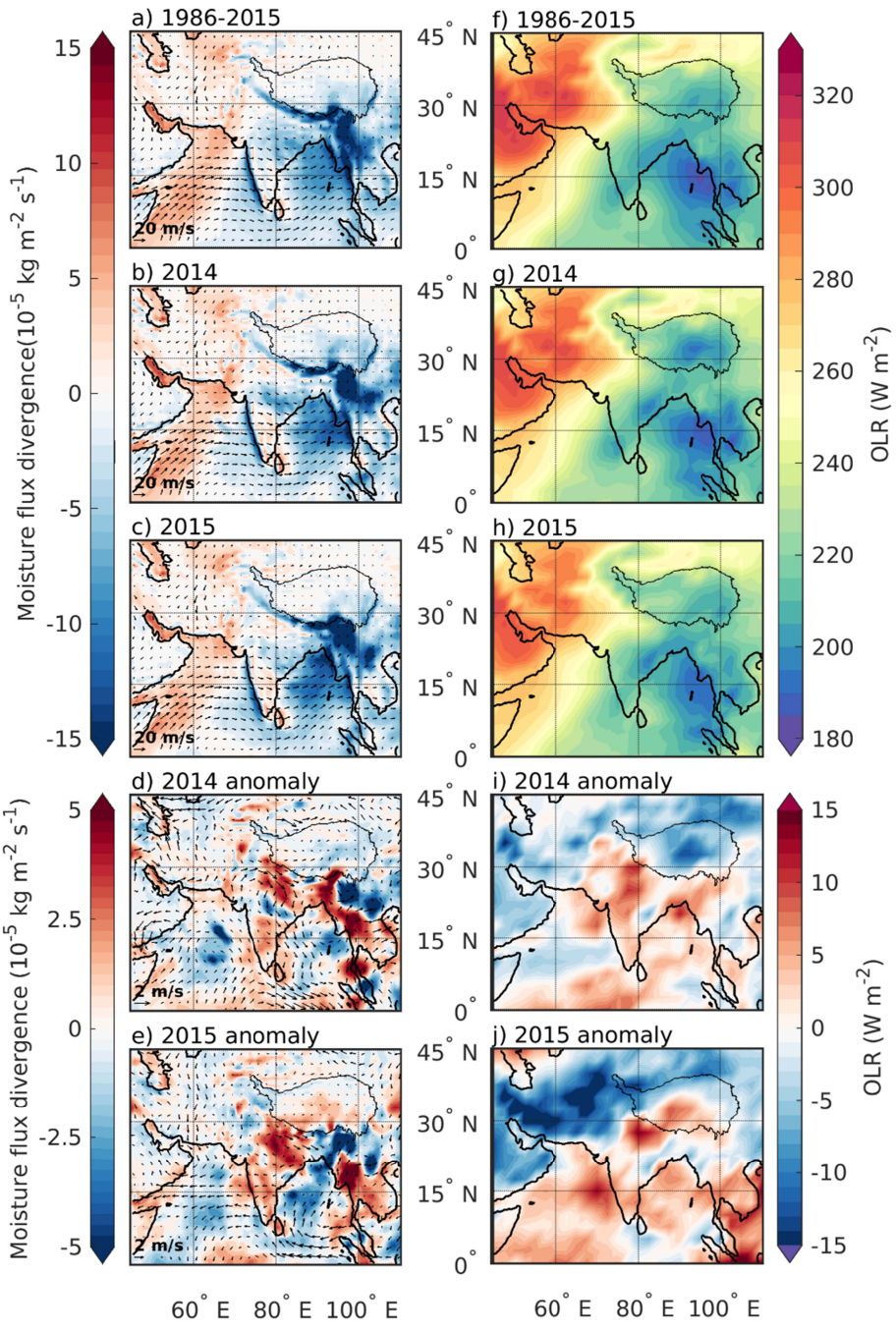

375

376 **Figure 6.** Vertically integrated moisture flux divergence and horizontal wind at the 850 hPa (left
377 pane) and outgoing longwave radiation (right pane) for monsoon seasons of (a, f) 1986-2015, (b,
378 g) 2014, (c, h) 2015, and anomalies of monsoons seasons of (d, i) 2014 and (e, j) 2015 relative to
379 relative to 1986-2015 mean.

380

Similar to the differences in E-P between 2014 and 2015 (Fig. 4 and 5), the spatial patterns of both moisture flux and zonal wind in JJAS 2014 differ from those in 2015 (Fig. 6d, e). An anomalous anticyclone pattern is found in central India in 2014, relative to JJAS 1986-2015, while 2015 experienced less change in the wind over the Indian continent. Opposite flux patterns appear over the BoB and Bangladesh between JJAS 2014 and 2015, indicating changes in moisture supplies along the moisture transport path to the southern TP. The wind anomalies in 2015 suggest a weakened monsoon over the western Indian Ocean, highlighted by the anomalous divergence over the west coast of India, and less convergence along the TP and the Himalayas.

Satellite-based measurements of OLR (Fig. 6f-j), a valuable proxy for deep atmospheric convection in the tropics (Evans & Webster, 2014; Krishnan et al., 2000; Zhang, 1993), relate to variations in precipitation stable isotopes (Risi et al., 2008). Figure 6f shows the OLR climatology (1986-2015), with the lowest values of <180 W/m^2 found in the eastern BoB, and the highest values of >300 W/m^2 over the Arabian Peninsula. Consistent with the convergence, and the threshold of 200 W/m^2 for deep convection in monsoon regions (Evans & Webster, 2014), substantial moisture uplift is evident in east India, Bangladesh, and the BoB (Fig. 6a, f). Negative OLR anomalies in 2015 appear in east India and Bangladesh, indicating stronger convection in these regions, while weaker convection over the BoB, South China Sea, and around Indonesia, may prevent moisture from reaching Yadong valley (Fig. 6j). Positive anomalies in the southern TP also reflect weaker convection than the climatology, which may cause increased evaporation resulting in enriched isotopes in vapor and precipitation. Lee et al. (2015) found that reduced convection in the eastern Indian Ocean results in enriched water vapor ^{18}O during El Niño. During El Niño events, the rising branch over the western Pacific weakens (Trenberth, 1997; Walker, 1925), which affects the BoB convection through teleconnections mediated by the Madden-Julian Oscillation (MJO, Madden & Julian, 1971; Zhang, 2005). The MJO enhances convection over the western Pacific and triggers the development of a high-pressure system, which can lead to a low-pressure system and drier conditions in the BoB (Anandh et al., 2018). El Niño events, alone or in conjunction with other climate patterns such as a positive Indian Ocean Dipole, can exacerbate the impacts on the BoB by enhancing the active phase of the MJO (Zhang et al., 2021). The influence of ENSO on precipitation stable isotopes in the southern TP was also identified in the 2005-2007 El Niño and La Niña years through changes

in convective activities and changes to the moisture transport (Gao et al., 2018; Lee et al., 2015; Cai & Tian, 2016). Our results further suggest that El Niño modulated the evaporation and convective activities over the BoB and Indian Peninsula, resulting in changes in moisture supplies along the transport paths to the central Himalayas and Yadong Valley.

4 Conclusions

In this study, we presented event-based precipitation stable isotope measurements from Yadong and Pali stations in the central Himalayas during 2014-2015 and simulations of moisture transport using the FLEXPART model. The spatiotemporal variations of E-P from north-eastern India, the Arabian Sea, and Bangladesh associated with depleted/increased $\delta^{18}O$ and d-excess in precipitation in the Yadong valley in 2015, highlight the importance of changes to evaporation and convective activities along the moisture transport paths for monthly variations in the precipitation stable isotopes. Our findings suggest that the 2015 El Niño event may have contributed to these changes by transferring moisture supplies into losses in eastern India and weakening the convective activities over the BoB. In addition, the typical negative lapse rate in $\delta^{18}O$ reversed in 2015, while the local temperature and precipitation amount effects were minimal.

Although limited by a short sampling period, our results provide valuable insights into the moisture supplies and losses along the transport paths from the Arabian Sea and the BoB to the central Himalayas. We also caution against relying solely on precipitation stable isotope archives to infer past temperature or precipitation variability in this region, given the potential influence of the El Niño effect on the isotopic composition of precipitation. Further investigations are needed to better understand the mechanisms driving the observed changes in precipitation stable isotopes at inter-annual to decadal scale.

Acknowledgments

GJ was supported by the Natural Science Foundation of China (nos. 41988101-03 and 41922002), JA and QZ were supported by the Swedish Research Council (Vetenskapsrådet; grant nos. 2013-06476 and 2017-04232 to QZ), SE and MC were supported by the Norwegian research council (Forskningsrådet, KEYCLIM; grant no. 295046), and DC was supported by the Swedish Research Council Formas (grant no. 2017-01408). Parts of computations running FLEXPART were enabled by resources provided by the Swedish National Infrastructure for Computing (SNIC) at the National Supercomputer Centre (NSC), partially funded by the Swedish Research Council through grant agreement no. 2018-05973.

We acknowledge the staff at Tibetan observation stations for collecting the precipitation samples and for taking simultaneous notes, the staff at the Institute of Tibetan Plateau Research for measuring the samples, as well as Jesper Sjolte and Fangyuan Lin for helpful advice, comments, and discussion on text and figures.

Data Availability Statement

The sampled data of precipitation stable isotopes, temperature, and precipitation will be made available at the National Tibetan Plateau/Third Pole Environment Data Center (TPDC) after the manuscript is accepted for publication. ERA-interim data can be downloaded from https://www.ecmwf.int/en/forecasts/dataset/ecmwf-reanalysis-interim (last accessed: 2022-12-22, Dee et al., 2011). Daily interpolated outgoing longwave radiation data can be retrieved from https://psl.noaa.gov/data/gridded/data.olrcdr.interp.html (last accessed: 2022-12-22, Liebmann & Smith, 1996). The ETOPO1 dataset is found at https://www.ncei.noaa.gov/access/metadata/landing-page/bin/iso?id=gov.noaa.ngdc.mgg.dem:316 (last accessed: 2022-12-22, Amante & Eakins, 2009; NOAA National Geophysical Data Center, 2009). FLEXPART model and documentation can be found at https://www.flexpart.eu/ (last accessed: 2022-12-22, Pisso et al., 2019).

Author Contributions

Conceptualization: JA and JG; Methodology: JA, JG, SE and MC; Data curation: JA, JG, SE and MC; Formal analysis: JA; Visualization: JA; Resources: JG, SE, MC, and QZ; Funding

464 acquisition: JG, SE, MC, DC and QZ; Writing – original draft: JA and JG; Writing – review &
465 editing: JA, JG, SE, MC, DC and QZ

References

Acharya, S., Yang, X., Yao, T., & Shrestha, D. (2020). Stable isotopes of precipitation in Nepal Himalaya highlight the topographic influence on moisture transport. *Quaternary International*, *565*, 22–30. https://doi.org/10.1016/j.quaint.2020.09.052

Adhikari, N., Gao, J., Yao, T., Yang, Y., & Dai, D. (2020). The main controls of the precipitation stable isotopes at Kathmandu, Nepal. *Tellus, Series B: Chemical and Physical Meteorology*, *72*(1), 1–17. https://doi.org/10.1080/16000889.2020.1721967

Amante, C., & Eakins, B. W. (2009). *ETOPO1 1 Arc-Minute Global Relief Model: Procedures, Data Sources and Analysis*. NOAA Technical Memorandum NESDIS NGDC-24. National Geophysical Data Center, NOAA. https://doi.org/10.7289/V5C8276M

Ambach, W., Dansgaard, W., Eisner, H., & Møller, J. (1968). The altitude effect on the isotopic composition of precipitation and glacier ice in the Alps. *Tellus*, *20*(4), 595–600. https://doi.org/10.3402/tellusa.v20i4.10040

Anandh, P. C., Vissa, N. K., & Broderick, C. (2018). Role of MJO in modulating rainfall characteristics observed over India in all seasons utilizing TRMM. *International Journal of Climatology*, *38*(5), 2352–2373. https://doi.org/10.1002/JOC.5339

Ananthakrishnan, R. (1970). Reversal of pressure gradients and wind circulation across India and the southwest monsoon. *Quarterly Journal of the Royal Meteorological Society*, *96*(409), 539–542. https://doi.org/10.1002/QJ.49709640915

Araguás-Araguás, L., Froehlich, K., & Rozanski, K. (2000). Deuterium and oxygen-18 isotope composition of precipitation and atmospheric moisture. *Hydrological Processes*, *14*(8), 1341–1355. https://doi.org/10.1002/1099-1085(20000615)14:8<1341::AID-HYP983>3.0.CO;2-Z

Bershaw, J. (2018). Controls on Deuterium Excess across Asia. *Geosciences*, *8*(7), 257. https://doi.org/10.3390/geosciences8070257

Cai, Z., & Tian, L. (2016). Atmospheric controls on seasonal and interannual variations in the precipitation isotope in the East Asian Monsoon region. *Journal of Climate*, *29*(4), 1339–1352. https://doi.org/10.1175/JCLI-D-15-0363.1

Cai, Z., Tian, L., & Bowen, G. J. (2017). ENSO variability reflected in precipitation oxygen isotopes across the Asian Summer Monsoon region. *Earth and Planetary Science Letters*, *475*, 25–33. https://doi.org/10.1016/j.epsl.2017.06.035

Chen, B., Xu, X.-D., Yang, S., & Zhang, W. (2012). On the origin and destination of atmospheric moisture and air mass over the Tibetan Plateau. *Theoretical and Applied Climatology*, *110*(3), 423–435. https://doi.org/10.1007/s00704-012-0641-y

Chen, K., Axelsson, J., Zhang, Q., Li, J., & Wang, L. (2022). EC-Earth simulations reveal enhanced inter-hemispheric thermal contrast during the Last Interglacial further intensified the Indian Monsoon. *Geophysical Research Letters*, *49*(6), 1–9. https://doi.org/10.1029/2021gl094551

Chhetri, T. B., Yao, T., Yu, W., Ding, L., Joswiak, D., Tian, L., Devkota, L. P., & Qu, D. (2014). Stable isotopic compositions of precipitation events from Kathmandu, southern slope of the Himalayas. *Chinese Science Bulletin*, *59*(34), 4838–4846. https://doi.org/10.1007/s11434-014-0547-4

Clark, C. O., Cole, J. E., & Webster, P. J. (2000). Indian Ocean SST and Indian summer rainfall: Predictive relationships and their decadal variability. *Journal of Climate*, *13*(14), 2503–2519. https://doi.org/10.1175/1520-0442(2000)013<2503:IOSAIS>2.0.CO;2

Clark, I. D., & Fritz, P. (1997). *Environmental isotopes in hydrogeology*. CRC Press/Lewis Publishers.

Craig, H. (1961). Isotopic Variations in Meteoric Waters. *Science*, *133*(3465), 1702–1703. https://doi.org/10.1126/science.133.3465.1702

Dai, D., Gao, J., Steen-Larsen, H. C., Yao, T., Ma, Y., Zhu, M., & Li, S. (2021). Continuous monitoring of the isotopic composition of surface water vapor at Lhasa, southern Tibetan Plateau. *Atmospheric Research*, *264*, 105827. https://doi.org/10.1016/J.ATMOSRES.2021.105827

Dansgaard, W. (1964). Stable isotopes in precipitation. *Tellus*, *16*(4), 436–468. https://doi.org/10.3402/tellusa.v16i4.8993

Dee, D. P., Uppala, S. M., Simmons, A. J., Berrisford, P., Poli, P., Kobayashi, S., Andrae, U., Balmaseda, M. A., Balsamo, G., Bauer, P., Bechtold, P., Beljaars, A. C. M., van de Berg, L., Bidlot, J., Bormann, N., Delsol, C., Dragani, R., Fuentes, M., Geer, A. J.,

Haimberger, L., Healy, S. B., Hersbach, H., Hólm, E. V., Isaksen, L., Kållberg, P., Köhler, M., Matricardi, M., McNally, A. P., Monge-Sanz, B. M., Morcrette, J.-J., Park, B.-K., Peubey, C., de Rosnay, P., Tavolato, C., Thépaut, J.-N. & Vitart, F. (2011). The ERA-Interim reanalysis: Configuration and performance of the data assimilation system. *Quarterly Journal of the Royal Meteorological Society*, *137*(656), 553-597. doi:10.1002/qj.828

Ding, Y., & Chan, J. C. L. (2005). The East Asian summer monsoon: An overview. In *Meteorology and Atmospheric Physics* (Vol. 89, Issues 1–4, pp. 117–142). Springer-Verlag. https://doi.org/10.1007/s00703-005-0125-z

Drumond, A., Nieto, R., & Gimeno, L. (2011). Sources of moisture for China and their variations during drier and wetter conditions in 2000-2004: A Lagrangian approach. *Climate Research*, *50*(2–3), 215–225. https://doi.org/10.3354/cr01043

Evans, J. L., & Webster, C. C. (2014). A variable sea surface temperature threshold for tropical convection. *Australian Meteorological and Oceanographic Journal*, *64*(March 2014), S1–S8. https://doi.org/10.22499/2.6401.007

Feng, L., & Zhou, T. (2012). Water vapor transport for summer precipitation over the Tibetan Plateau: Multidata set analysis. *Journal of Geophysical Research Atmospheres*, *117*(20). https://doi.org/10.1029/2011JD017012

Gao, J., Yao, T., Masson-Delmotte, V., Steen-Larsen, H. C. & Wang, W. (2019). Collapsing glaciers threaten Asia's water supplies. *Nature*, *565*(7737), 19–21. https://doi.org/10.1038/d41586-018-07838-4

Gao, J., He, Y., Masson-Delmotte, V., & Yao, T. (2018). ENSO effects on annual variations of summer precipitation stable isotopes in Lhasa, southern Tibetan Plateau. *Journal of Climate*, *31*(3), 1173–1182. https://doi.org/10.1175/JCLI-D-16-0868.1

Gao, J., Masson-Delmotte, V., Yao, T., Tian, L., Risi, C., & Hoffmann, G. (2011). Precipitation water stable isotopes in the South Tibetan plateau: Observations and modeling. Journal of Climate, 24(13), 3161–3178. https://doi.org/10.1175/2010JCLI3736.1

Gao, J., Masson-Delmotte, V., Risi, C., He, Y., & Yao, T. (2013). What controls precipitation δ18O in the southern Tibetan Plateau at seasonal and intra-seasonal

556 scales? A case study at Lhasa and Nyalam. *Tellus B: Chemical and Physical*
557 *Meteorology*, *65*(1), 21043. https://doi.org/10.3402/tellusb.v65i0.21043
558 Gao, J., Risi, C., Masson-Delmotte, V., He, Y., & Xu, B. (2016). Southern Tibetan Plateau
559 ice core δ18O reflects abrupt shifts in atmospheric circulation in the late 1970s.
560 *Climate Dynamics*, *46*(1–2), 291–302. https://doi.org/10.1007/s00382-015-2584-3
561 Gao, J., Shen, S. S. P. P., Yao, T., Tafolla, N., Risi, C., & He, Y. (2015). Reconstruction of
562 precipitation δ18O over the Tibetan plateau since 1910. *Journal of Geophysical*
563 *Research*, *120*(10), 4878–4888. https://doi.org/10.1002/2015JD023233
564 Gao, Y., Cuo, L., & Zhang, Y. (2014). Changes in Moisture Flux over the Tibetan Plateau
565 during 1979–2011 and Possible Mechanisms. *Journal of Climate*, *27*(5), 1876–1893.
566 https://doi.org/10.1175/JCLI-D-13-00321.1
567 Gat, J. R. (1996). Oxygen and Hydrogen Isotopes in the Hydrologic Cycle. *Annual Review*
568 *of Earth and Planetary Sciences*, *24*(1), 225–262. https://doi.org/10.1007/s00170-012-
569 4640-z
570 Geng, T., Cai, W., Wu, L., Santoso, A., Wang, G., Jing, Z., Gan, B., Yang, Y., Li, S.,
571 Wang, S., Chen, Z., & McPhaden, M. J. (2022). Emergence of changing Central-
572 Pacific and Eastern-Pacific El Niño-Southern Oscillation in a warming climate. *Nature*
573 *Communications*, *13*(1), 6616. https://doi.org/10.1038/s41467-022-33930-5
574 Gimeno, L., Drumond, A., Nieto, R., Trigo, R. M., & Stohl, A. (2010). On the origin of
575 continental precipitation. *Geophysical Research Letters*, *37*(13), n/a-n/a.
576 https://doi.org/10.1029/2010GL043712
577 Gonfiantini, R., Roche, M. A., Olivry, J. C., Fontes, J. C., & Zuppi, G. M. (2001). The
578 altitude effect on the isotopic composition of tropical rains. *Chemical Geology*, *181*(1–
579 4), 147–167. https://doi.org/10.1016/S0009-2541(01)00279-0
580 Hahn, G. D., & Manabe, S. (1976). The Role of Mountains in the South Asian Monsoon
581 Circulation. *Journal of the Atmospheric Sciences*, *33*(11), 2255–2258.
582 https://doi.org/10.1175/1520-0469
583 Hao, Z., Hongcai, F., Lian, L., & Turner, S. (2013). Scientists Discuss the Genetic
584 Relationship between Qinghai-Tibet Plateau and Indian Monsoon. *Acta Geologica*
585 *Sinica - English Edition*, *87*(4), 1181–1182. https://doi.org/10.1111/1755-6724.12121

He, Y., Risi, C., Gao, J., Masson-Delmotte, V., Yao, T., Lai, C. T., Ding, Y., Worden, J., Frankenberg, C., Chepfer, H., & Cesana, G. (2015). Impact of atmospheric convection on south Tibet summer precipitation isotopologue composition using a combination of in situ measurements, satellite data, and atmospheric general circulation modeling. *Journal of Geophysical Research*, *120*(9), 3852–3871. https://doi.org/10.1002/2014JD022180

ICIMOD. (2021). *Regional Programme: River Basins and Cryosphere*. https://www.icimod.org/regional-programme/river-basins-and-cryosphere

Kakatkar, R., Gnanaseelan, C., Chowdary, J. S., Parekh, A., & Deepa, J. S. (2018). Indian summer monsoon rainfall variability during 2014 and 2015 and associated Indo-Pacific upper ocean temperature patterns. *Theoretical and Applied Climatology*, *131*(3–4), 1235–1247. https://doi.org/10.1007/s00704-017-2046-4

Kripalani, R. H., & Kulkarni, A. (1997). Climatic impact of El Niño/La Niña on the Indian monsoon: A new perspective. *Weather*, *52*(2), 39–46. https://doi.org/10.1002/j.1477-8696.1997.tb06267.x

Krishnan, R., Zhang, C., & Sugi, M. (2000). Dynamics of Breaks in the Indian Summer Monsoon. *Journal of the Atmospheric Sciences*, *57*(9), 1354–1372. https://doi.org/10.1175/1520-0469(2000)057<1354:DOBITI>2.0.CO;2

Kumar, K. K., Rajagopalan, B., Hoerling, M., Bates, G., & Cane, M. (2006). Unraveling the mystery of Indian monsoon failure during El Niño. *Science*, *314*(5796), 115–119. https://doi.org/10.1126/science.1131152

Lee, J., Worden, J., Noone, D., Chae, J. H., & Frankenberg, C. (2015). Isotopic changes due to convective moistening of the lower troposphere associated with variations in the ENSO and IOD from 2005 to 2006. *Tellus, Series B: Chemical and Physical Meteorology*, *67*(1). https://doi.org/10.3402/tellusb.v67.26177

Liebmann, B., & Smith, C. A. (1996). Description of a Complete (Interpolated) Outgoing Longwave Radiation Dataset. *Bulletin of the American Meteorological Society*, *77*(6), 1275–1277. http://www.jstor.org/stable/26233278

Madden, R. A., & Julian, P. R. (1971). Detection of a 40–50 day oscillation in the zonal wind in the tropical Pacific. *Journal of the Atmospheric Sciences*, *28*, 702–708.

https://journals.ametsoc.org/view/journals/atsc/28/5/1520-0469_1971_028_0702_doadoi_2_0_co_2.xml

Mekonnen, A., Renwick, J. A., Sánchez-Lugo, A., & Eds. (2016). South Asia [in "State of the Climate 2015"]. *Bulletin of the American Meteorological Society*, *97*(8), S215–S216.

Merlivat, L., & Jouzel, J. (1979). Global climatic interpretation of the deuterium-oxygen 18 relationship for precipitation. *Journal of Geophysical Research*, *84*(C8), 5029–5033. https://doi.org/10.1029/JC084iC08p05029

Michel, C., Sorteberg, A., Eckhardt, S., Weijenborg, C., Stohl, A., & Cassiani, M. (2021). Characterization of the atmospheric environment during extreme precipitation events associated with atmospheric rivers in Norway-Seasonal and regional aspects. *Weather and Climate Extremes*, *34*, https://doi.org/10.1016/j.wace.2021.100370

NOAA National Geophysical Data Center. (2009). ETOPO1 1 Arc-Minute Global Relief Model [Dataset]. NOAA National Centers for Environmental Information. https://doi.org/10.7289/V5C8276M

Nogueira, M. (2020). Inter-comparison of ERA-5, ERA-interim and GPCP rainfall over the last 40 years: Process-based analysis of systematic and random differences. *Journal of Hydrology*, *583*, 124632. https://doi.org/10.1016/j.jhydrol.2020.124632

Pisso, I., Sollum, E., Grythe, H., Kristiansen, N. I., Cassiani, M., Eckhardt, S., Arnold, D., Morton, D., Thompson, R. L., Groot Zwaaftink, C. D., Evangeliou, N., Sodemann, H., Haimberger, L., Henne, S., Brunner, D., Burkhart, J. F., Fouilloux, A., Brioude, J., Philipp, A., Seibert, P. & Stohl, A. (2019). The Lagrangian particle dispersion model FLEXPART version 10.4. *Geoscientific Model Development*, *12*(12), 4955–4997. https://doi.org/10.5194/gmd-12-4955-2019

Power, K., Axelsson, J., Wangdi, N., & Zhang, Q. (2021). Regional and local impacts of the ENSO and IOD events of 2015 and 2016 on the Indian summer monsoon—A bhutan case study. *Atmosphere*, *12*(8), 954. https://doi.org/10.3390/atmos12080954

Ren, W., Yao, T., Xie, S., & He, Y. (2017). Controls on the stable isotopes in precipitation and surface waters across the southeastern Tibetan Plateau. *Journal of Hydrology*, *545*, 276–287. https://doi.org/10.1016/j.jhydrol.2016.12.034

Risi, C., Bony, S., & Vimeux, F. (2008). Influence of convective processes on the isotopic composition (δ18O and δD) of precipitation and water vapor in the tropics: 2. Physical interpretation of the amount effect. *Journal of Geophysical Research Atmospheres*, *113*(19), D19306. https://doi.org/10.1029/2008JD009943

Rozanski, K., Araguás-Araguás, L., & Gonfiantini, R. (1993). Isotopic Patterns in Modern Global Precipitation. In *Climate Change in Continental Isotopic Records* (pp. 1–36). American Geophysical Union (AGU). https://doi.org/10.1029/GM078p0001

Rozanski, K., Araguás-Araguás, L., Gonfiantini, R., Araguãs-Araguãs, L., & Gonfiantini, R. (1992). Relation Between Long-Term Trends of Oxygen-18 Isotope Composition of Precipitation and Climate. *Science*, *258*(5084), 981–985. https://doi.org/10.1126/science.258.5084.981

Sodemann, H., & Stohl, A. (2013). Moisture Origin and Meridional Transport in Atmospheric Rivers and Their Association with Multiple Cyclones*. *Monthly Weather Review*, *141*(8), 2850–2868. https://doi.org/10.1175/MWR-D-12-00256.1

Srivastava, G., Chakraborty, A., & Nanjundiah, R. S. (2019). Multidecadal see-saw of the impact of ENSO on Indian and West African summer monsoon rainfall. *Climate Dynamics*, *52*(11), 6633–6649. https://doi.org/10.1007/s00382-018-4535-2

Stohl, A., Forster, C., & Sodemann, H. (2008). Remote sources of water vapor forming precipitation on the Norwegian west coast at 60°N-a tale of hurricanes and an atmospheric river. *Journal of Geophysical Research: Atmospheres*, *113*(D5), n/a-n/a. https://doi.org/10.1029/2007JD009006

Stohl, A., Hittenberger, M., & Wotawa, G. (1998). Validation of the Lagrangian particle dispersion model FLEXPART against large-scale tracer experiment data. *Atmospheric Environment*, *32*(24), 4245–4264. https://doi.org/10.1016/S1352-2310(98)00184-8

Stohl, A., & James, P. (2004). A Lagrangian Analysis of the Atmospheric Branch of the Global Water Cycle. Part I: Method Description, Validation, and Demonstration for the August 2002 Flooding in Central Europe. *Journal of Hydrometeorology*, *5*(4), 656–678. https://doi.org/10.1175/1525-7541(2004)005<0656:ALAOTA>2.0.CO;2

Stohl, A., & James, P. (2005). A Lagrangian Analysis of the Atmospheric Branch of the Global Water Cycle. Part II: Moisture Transports between Earth's Ocean Basins and

River Catchments. *Journal of Hydrometeorology*, *6*(6), 961–984. https://doi.org/10.1175/JHM470.1

Sun, B., & Wang, H. (2014). Moisture Sources of Semiarid Grassland in China Using the Lagrangian Particle Model FLEXPART. *Journal of Climate*, *27*(6), 2457–2474. https://doi.org/10.1175/JCLI-D-13-00517.1

Tian, L., Masson-Delmotte, V., Stievenard, M., Yao, T., & Jouzel, J. (2001). Tibetan Plateau summer monsoon northward extent revealed by measurements of water stable isotopes. *Journal of Geophysical Research Atmospheres*, *106*(D22), 28081–28088. https://doi.org/10.1029/2001JD900186

Tian, L., Tandong, Y., White, J. W. C., Wusheng, Y., & Ninglian, W. (2005). Westerly moisture transport to the middle of Himalayas revealed from the high deuterium excess. *Chinese Science Bulletin*, *50*(10), 1026. https://doi.org/10.1360/04wd0030

Torrence, C., & Webster, P. J. (1999). Interdecadal changes in the ENSO-monsoon system. *Journal of Climate*, *12*(8 PART 2), 2679–2690. https://doi.org/10.1175/1520-0442(1999)012<2679:icitem>2.0.co;2

Trenberth, K. E. (1997). The definition of El Niño. *Bulletin of the American Meteorological Society*, *78*(12), 2771–2777. https://doi.org/10.1175/1520-0477(1997)078<2771:TDOENO>2.0.CO;2

Trenberth, K. E., Dai, A., Rasmussen, R. M., & Parsons, D. B. (2003). The Changing Character of Precipitation. *Bulletin of the American Meteorological Society*, *84*(9), 1205–1217. https://doi.org/10.1175/BAMS-84-9-1205

Walker, G. T. (1925). Correlation in seasonal variations of weather - A further study of world weather. *Monthly Weather Review*, *53*(6), 252–254. https://doi.org/10.1175/1520-0493(1925)53<252:cisvow>2.0.co;2

Wang, D., Tian, L., Cai, Z., Shao, L., Guo, X., Tian, R., Li, Y., Chen, Y., & Yuan, C. (2020). Indian monsoon precipitation isotopes linked with high level cloud cover at local and regional scales. *Earth and Planetary Science Letters*, *529*, 115837. https://doi.org/10.1016/j.epsl.2019.115837

Wang, Z. & Chang, C. P. (2012). A Numerical Study of the Interaction between the Large-Scale Monsoon Circulation and Orographic Precipitation over South and Southeast

706 Asia. *Journal of Climate*, *25*(7), 2440–2455. https://doi.org/10.1175/JCLI-D-11-
707 00136.1
708 Webster, P. J. (1995). Meteorology and Atmospheric Physics The Annual Cycle and the
709 Predictability of the Tropical Coupled Ocean-Atmosphere System. In *Meteorol. Atmos.*
710 *Phys* (Vol. 56).
711 Wu, R.-G., Hu, K.-M., & Lin, Z.-D. (2017). Relationship between Indian and East Asian
712 summer rainfall variations. *Advances in Atmospheric Sciences*, *34*(1), 4–15.
713 https://doi.org/10.1007/s00376-016-6216-6
714 Ya, G., Huijun, W., & Shuanglin, L. (2013). Influences of the Atlantic Ocean on the
715 summer precipitation of the southeastern Tibetan Plateau. *Journal of Geophysical*
716 *Research: Atmospheres*, *118*(9), 3534–3544. https://doi.org/10.1002/jgrd.502902013
717 Yao, T., Masson-Delmotte, V., Gao, J., Yu, W., Yang, X., Risi, C., Sturm, C., Werner, M.,
718 Zhao, H., He, Y., Ren, W., Tian, L., Shi, C., & Hou, S. (2013). A review of climatic
719 controls on δ18O in precipitation over the Tibetan Plateau: Observations and
720 simulations. *Reviews of Geophysics*, *51*(4), 525–548. https://doi.org/10.1002/rog.20023
721 Yu, W., Yao, T., Tian, L., Ma, Y., Wen, R., Devkota, L. P., Wang, W., Qu, D., & Chhetri,
722 T. B. (2016). Short-term variability in the dates of the Indian monsoon onset and retreat
723 on the southern and northern slopes of the central Himalayas as determined by
724 precipitation stable isotopes. *Climate Dynamics*, *47*(1–2), 159–172.
725 https://doi.org/10.1007/s00382-015-2829-1
726 Zhang, C. (1993). Large-Scale Variability of Atmospheric Deep Convection in Relation to
727 Sea Surface Temperature in the Tropics. *Journal of Climate*, *6*(10), 1898–1913.
728 https://doi.org/10.1175/1520-0442(1993)006<1898:LSVOAD>2.0.CO;2
729 Zhang, C., Tang, Q., & Chen, D. (2017). Recent Changes in the Moisture Source of
730 Precipitation over the Tibetan Plateau. *Journal of Climate*, *30*(5), 1807–1819.
731 https://doi.org/10.1175/JCLI-D-15-0842.1
732 Zhang, C. (2005). Madden-Julian Oscillation. *Reviews of Geophysics*, *43*(2), 1–36.
733 https://doi.org/10.1029/2004RG000158
734 Zhang, L., Han, W., & Hu, Z. Z. (2021). Interbasin and Multiple-Time-Scale Interactions in
735 Generating the 2019 Extreme Indian Ocean Dipole. *Journal of Climate*, *34*(11), 4553–
736 4566. https://doi.org/10.1175/JCLI-D-20-0760.1

737